AD-A106 569 FOREST PRODUCTS LAB MADISON WI F/G 13/4
OVERALL EFFECTIVE THERMAL RESISTANCE OF CORRUGATED FIBERBOARD C--ETC(U)
AUG 81 D W BORMETT
UNCLASSIFIED FSRP-FPL-406 NL

1 OF 1
AD A106 569

END
DATE FILMED
11-81
DTIC

United States
Department of
Agriculture

Forest Service

Forest
Products
Laboratory

Research
Paper
FPL 406

Overall Effective Thermal Resistance of Corrugated Fiberboard Containers.

(12)

LEVEL II

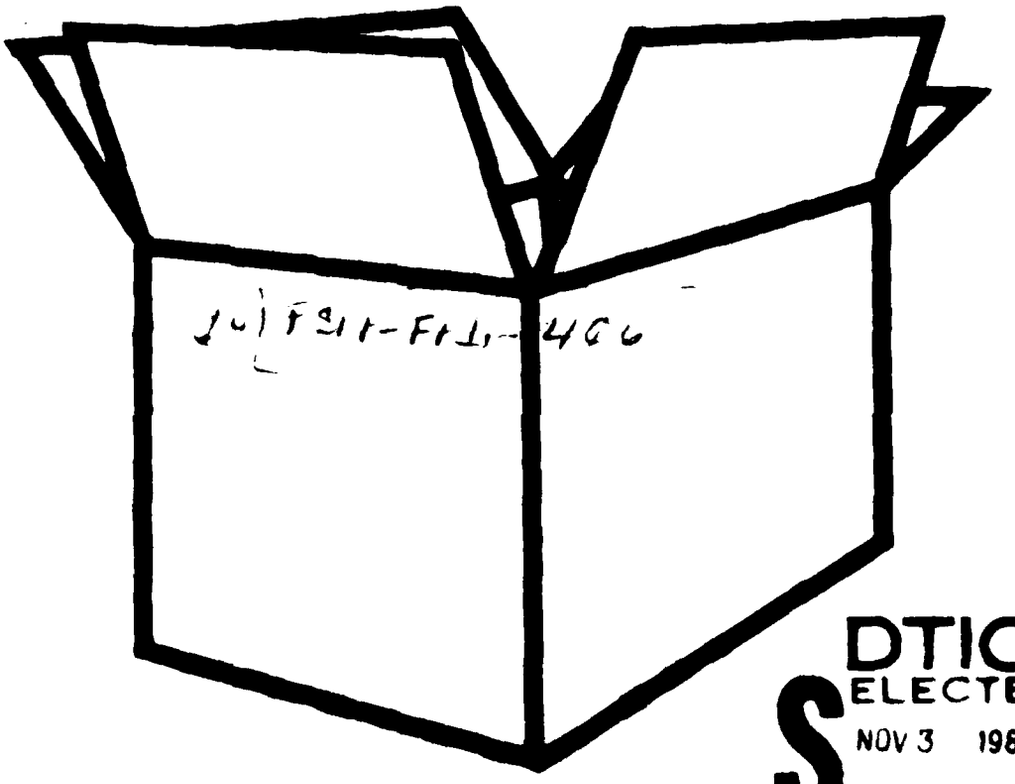

Abstract

The overall effective thermal resistance of a corrugated fiberboard container was determined as a function of air velocity and board thickness, and an appropriate design curve is presented. The thermal resistance of the container is treated as a sum of resistances, with individual resistance values presented for the interior interfacial contact resistance, the board resistance, and the exterior boundary resistance. Behavioral differences were found for heating versus cooling at conventional board thicknesses and a possible explanation for this behavior is presented.

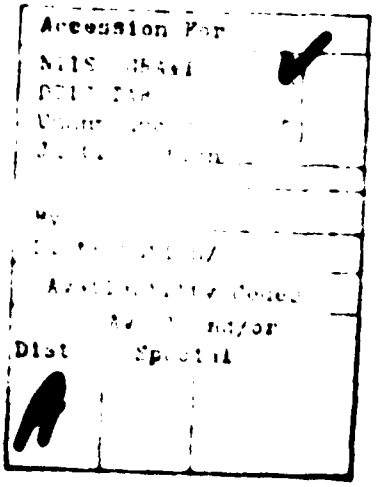

United States
Department of
Agriculture

Forest Service

Forest
Products
Laboratory[1]

Research
Paper
FPL 408

August 1981

Overall Effective Thermal Resistance of Corrugated Fiberboard Containers

By
DAVID W. BORMETT, Chemical Engineer

Introduction

Over the years of its development, the properties of corrugated fiberboard have been studied extensively in order to predict its behavior in usage. As these properties became better understood the corrugated container took the place of the wood box for general use. Packaging has now evolved to the point where the corrugated container is the primary packaging material.

However, despite the generation of a broad data base on the mechanical properties of corrugated fiberboard, little indepth research has been undertaken on its nonmechanical properties. In particular, even though the agricultural industry ships vast quantities of produce in corrugated boxes, little knowledge is available on the thermal properties of the corrugated container. While shipping and storing produce and frozen foods has been studied extensively, research emphasis has generally been on the carried product, with only mild consideration given to the package itself. Consequently, it is difficult to extract from the literature any design criteria for the thermal properties of corrugated boxes.

Ramaker[2] did determine the thermal resistance and conductivity of ovendry board as a function of board thickness and components and, based on these results, he generated a mathematical model to predict its thermal resistance. While the thermal resistance values are correct, the use of these values alone proved inadequate for predicting the actual thermal performance of boxes in use. Other controlling factors needed to be coupled with the thermal resistance to describe the box behavior.

As a result, this study was undertaken to determine the overall effective thermal resistance of a corrugated fiberboard container. The factors considered were board thickness, air velocity around the box, and direction of the thermal flux (inward or outward heat flow per unit area per unit time).

Procedure

Techniques exist for predicting the time-temperature behavior of a product packed in a corrugated fiberboard box. The user of these techniques is required to know (1) the geometry of the product; (2) its thermal characteristics of specific heat, density, and thermal conductivity; (3) the external bulk air environment in which the heating or cooling occurs; and (4) the thermal behavior between the product and the bulk air. It is first necessary to understand the conditions satisfying the first three requirements in actual use and to see how these conditions were simulated experimentally.

Requirements 1, 2, 3

While the thermal and geometric properties of a product are critical to any analysis (requirements 1 and 2), the diversity of products is so extensive that any amount of consideration of these variables would still be incomplete. Therefore, in this study product variables were kept constant by employing only one commercial product in one standard size, namely 454-gram flatpacks of margarine.

For requirement 3, from the user's standpoint two common bulk air environments are generally encountered:

---

[1] Maintained at Madison, Wis., with the cooperation of the University of Wisconsin.

[2] Ramaker, T. J. Thermal Resistance of Corrugated Fiberboard. Tappi 57(8):69-72, 1974.

(1) The package at a given temperature is placed in a constant-temperature room at a different temperature and at a very low circulating air flow rate such that the package is subjected primarily to convection currents; (2) high-velocity air at a temperature different than the package strikes the package on a single face and flows around it. A third situation frequently arising is air flowing through boxes by means of vent holes. This special case is being evaluated as a separate problem to be reported on at a later date. In this study the air flow patterns used were intended to simulate the above two common environments.

Requirement 4

Having set the conditions for the first three requirements, one can then consider the fourth requirement. A commercial packer or user is rarely concerned with the container but only with the product inside. In this respect the container serves as part of the overall resistance to the flow of heat between the product and bulk air.

Consider the package as being three separate thermal resistance zones through which heat must pass: (1) An interfacial contact resistance between the surface of the product and the inner surface of the corrugated fiberboard; (2) the resistance of the corrugated fiberboard itself; and (3) the resistance between the outer surface of the fiberboard and the bulk air. The sum of these three resistances is the overall effective thermal resistance of the package. Its reciprocal is the overall effective heat transfer coefficient.

To satisfy the fourth requirement a user must know the overall resistance, which, unfortunately, changes with both time and point-by-point location on the box. The changes are due to the heterogeneous contact between box and product, with the thickness of the fiberboard on each side of the box, and with the turbulent air profile surrounding the box.

While a strict analysis would take each of these factors into account, the results would be overly cumbersome for general field use. Thus, this work is an attempt to simplify the overall time-position resistance history into a single-value, approximate resistance characterizing the overall effective thermal behavior of the package. For additional theoretical considerations see Appendix I.

The actual technique for using the resultant resistance values for field use prediction of a time-temperature history on an arbitrarily sized container having an arbitrary product will be published in a subsequent report.

Summary of Experimental Procedure

Sets of four 454-gram (g) packs of commercial flatpack margarine were stacked in a 130- x 130- x 130-millimeter (mm) cube and packaged in corrugated fiberboard containers. Board thickness ranged from 0.33 mm (linerboard only) to 51 mm of built-up corrugated fiberboard. The various packages were subjected to heating/cooling periods at bulk air velocities of 0, 1.8, 3.6, and 5.4 meters per second (m/s). Instantaneous overall heat transfer coefficients were determined at the center point of each side of the package at frequent intervals for the duration of the temperature change. For each environmental condition, an overall time and position average effective heat transfer coefficient (U) was calculated for each package as a whole. The resulting coefficients are presented in table 1 along with their reciprocals ($\frac{1}{U}$), which are the desired overall effective thermal resistances (R) (fig. 1). For the detailed Experimental Procedure, see Appendix II.

Table 1.—Overall effective heat transfer coefficients and thermal resistances of a cubical corrugated container

Air velocity	Board thickness	Heat transfer coefficients (U)	Thermal resistance (R = 1/U)
m/s	mm	W/K•m²	K•m²/W
		COOLING	
0	0	7.94	0.13
	.33	4.31	.23
	4.23	3.40	.29
	12.7	1.82	.55
	25.4	1.19	.84
	50.8	.91	1.10
1.8	0	31.66	.03
	.33	4.71	.21
	4.23	3.46	.29
	12.7	1.93	.52
	25.4	1.08	.93
	50.8	.91	1.10
3.6	0	52.38	.02
	.33	4.99	.20
	4.23	3.86	.26
	12.7	1.99	.50
	25.4	1.31	.77
	50.8	.91	1.10
5.4	0	56.01	.02
	.33	4.77	.21
	4.23	3.97	.25
	12.7	1.99	.50
	25.4	1.36	.73
	50.8	.85	1.17
∞	0	50.84	.02
	.33	4.82	.21
	4.23	3.74	.27
	12.7	1.99	.50
	25.4	1.31	.77
	50.8	.91	1.10

Results and Discussion

Satisfying requirement 3, the data (fig. 1) for no air flow (maximum resistance, line III) and infinite air flow (minimum resistance, line II) represent the primary design data. Values for 1.8, 3.6, and 5.4 m/s are omitted as they are sufficiently close to the infinite air velocity values.

The three lines of figure 1 represent three thermal resistance levels: The ovendry board-only resistance

Table 1.—Overall effective heat transfer coefficients and thermal resistances of a cubical corrugated container—con.

Air velocity	Board thickness	Heat transfer coefficients (U)	Thermal resistance (R = 1/U)
m/s	mm	W/K•m²	K•m²/W
		HEATING	
0	0	3.06	0.33
	.33	2.38	.42
	4.23	2.21	.45
	12.7	1.64	.61
	25.4	1.25	.80
	50.8	.91	1.10
1.8	0	7.21	.14
	.33	5.33	.19
	4.23	3.23	.31
	12.7	1.99	.50
	25.4	1.36	.73
	50.8	.96	1.04
3.6	0	6.70	.15
	.33	5.33	.19
	4.23	3.46	.29
	12.7	2.04	.49
	25.4	1.36	.73
	50.8	.96	1.04
5.4	0	7.83	.13
	.33	5.50	.18
	4.23	3.63	.28
	12.7	1.99	.50
	25.4	1.42	.70
	50.8	.96	1.04
∞	0	7.55	.13
	.33	5.56	.18
	4.23	3.52	.28
	12.7	1.99	.50
	25.4	1.36	.73
	50.8	.96	1.04

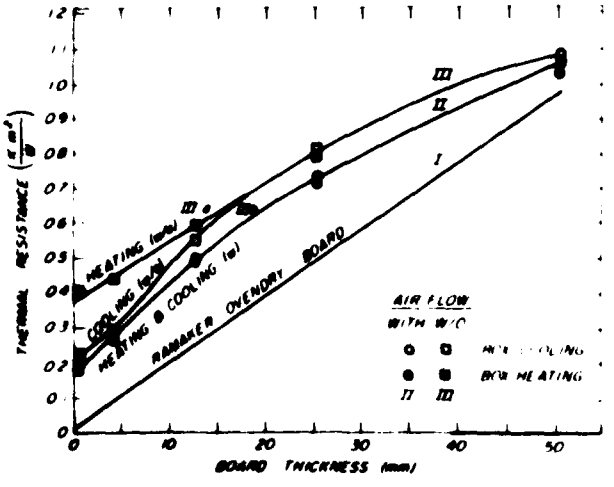

Figure 1.—Overall effective thermal resistance of a cubical corrugated container versus board thickness. Line I is resistance of ovendry board only. Line II is resistance of moist (10 pct moisture) board plus product-container interfacial resistance. Line III is resistance of moist board plus product-container interfacial resistance plus outer bulk air-container interfacial resistance. Line III-a is for heating of the container. Line III-b is for cooling the container.

(M 149721-8)

(line I), the board plus board-product interfacial resistance (line II), and the total overall resistance which includes the maximum outer bulk air-board interfacial resistance (line III).

Line I is taken from the equation[2] for ovendry corrugated fiberboard at a mean temperature of −1° C corresponding to the experimental mean temperature of this study. Lower resistance values than shown in line I may be in order due to moisture (5 to 10 pct) present in the board during the experimental runs. The extent of the deviation is not accurately known, but Ramaker presented evidence of a possible 15 to 80 percent decrease in resistance due to moisture. This effect is currently being investigated.

Line II represents the extrapolated zero-intercept values from table 2. These values are for infinite bulk air velocity, implying no outer bulk air-board boundary resistance exists. Only the board resistance and the board-product interfacial resistance remain. The shape of line II should be noted. Because the box and the solid have a tight fit, one would not expect convection at the interface. Nor should radiation be a significant factor due to the small temperature difference across the interface. Thus it would seem reasonable to expect a constant contact resistance at this interior interface, demonstrated by the parallelism of lines I and II. This is not the case as is emphasized by figure 2 (line II minus line I) which represents the interior interfacial contact resistance only. It remains to be determined if there is a true unexplained mechanism taking place or if the effect is merely scatter in the data. Regardless, one can assume that the board-product interfacial resistance for this system will be 0.18 to 0.27° Kelvin • square meters per watt (K•m²/W) at normal box thicknesses[3] of 2.5-20 mm. This implies a minimum overall combined resistance of three times that due to board alone. This means that the board resistance alone is not sufficient for calculating heating/cooling times for boxes and the inner and outer interfacial resistances must be included.

Figure 1, line III represents the overall effective resistance for no bulk air flow (stagnant air), that is, exterior convection effects only. The outer air boundary layer would have minimal disturbance, therefore maximum resistance. As with the difference between lines I and II, the difference between lines II and III is the actual thermal resistance of the outer boundary air layer. For board thicknesses greater than 20 mm the stagnant outer air resistance is nearly constant at 0.09 K•m²/W. However, in the normally used thickness range of less than 20 mm an obviously differing pattern exists. Heating versus cooling shows a distinct difference as shown by the splitting of line III. One possible explanation for this behavior can be found by considering the nature of the outer boundary air layer. A hypothesis of this behavior can be found in Appendix III.

[3] Typical thickness ranges for single-wall combined board are: 4.6-5.8 mm (A-flute), 3.8-4.8 mm (C-flute), and 2.8-3.8 mm (B-flute).

Table 2.—Determination of effective thermal resistance from air velocity[1,2]

Boxboard thickness	Flux direction	Resistance (K•m²/W) = a + (b/x)³	
		a	b
mm	Cooling/heating		
0.33 (kraft liner)	c	0.21	0.0023
	h	.18	.0206
4.2 (single wall)	c	.27	.0026
	h	.28	.0144
12.7	c	.50	.0049
	h	.50	.0096
25.4	c	.77	.0068
	h	.73	.0065
50.8	c	1.10	.0006
	h	1.04	.0027

[1] Constant "b" generated from linear regression of data of table 1, excluding data for infinite air velocity. Extrapolation of these regression lines to zero inverse air velocity gives the constant "a," corresponding to the infinite air velocity data included in table 1.

[2] Equations are valid for air velocities in the range 0.09 to 5.4 m/s. For velocities in the range 0.00 to 0.09 m/s use data for 0 m/s in table 1 or figure 1.

[3] The value "x" is the air velocity in meters per second.

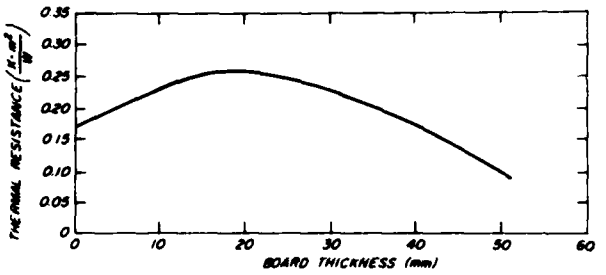

Figure 2 — Interior interfacial thermal resistance of the corrugated container-margarine system. These values will change with the nature of the interfacial contact of the product being packaged.

(M 149721-7)

While the proposed mechanism needs to be proved or disproved, the varying thermal behavior does exist in the region of common board thicknesses. Most significantly, the thermal resistance for a single-wall box during heating with no air movement except natural convection is 0.44 K•m²/W or five times the resistance of board alone. Again, this emphasizes the necessity of including the interfacial resistances in any calculations. Similarly with no forced air movement a thawing (heating) period may take considerably longer than a freezing (cooling) period as shown by the higher resistance (line III-a) for heating compared to the lower resistance (line III-b) for cooling.

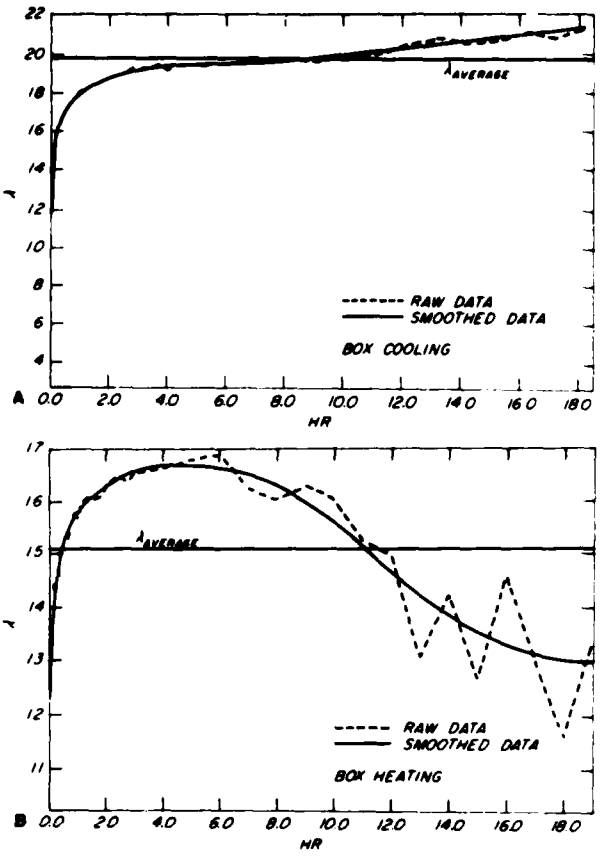

Figure 3 — Change with time of the overall effective heat transfer coefficient (U) as reflected by the first root (λ) of the equation $U/k = \lambda \tan \lambda L$. (A) cooling, (B) heating. Horizontal line is the average root found by integrating the area under the smoothed data and dividing by the total time.

((A) M 149721-6)
((B) M 149721-5)

At normal board thicknesses blast cooling of a box with no vent holes will have only marginal effects. Compare lines III-b and II in figure 1. Conversely, blast heating would be a definite asset to reducing heating or thawing times (line III-a minus line II).

Noting that the values of resistance reported here are average values calculated for temperature changes 90 percent or more complete, examination of figure 3 shows that if one were to abbreviate the heating/cooling period, the average value of λ, indicative of the reciprocal resistance, would be altered.

Conclusions

1. The overall effective thermal resistance of a corrugated fiberboard package is not constant but will vary from about 0.18 K•m²/W for a kraft linerboard package (0.33 mm thick) to about 1.16 K•m²/W for a corrugated fiberboard box having walls 51 mm thick.

2. The thermal resistance of the fiberboard is not a reasonable approximation of the total resistance. The

resistances of the box-product interface and of the outer boundary air layer are significant, adding 0.18-0.36 K•m²/W to the board resistance. For normal box thicknesses the total resistance will be 3-5 times that of board alone.

3. For a board thickness of less than 20 mm a distinct difference in heating and cooling behavior exists at very low bulk air velocities with heating periods being significantly greater than cooling periods on the same package.

Appendix I—Theory

General

An energy balance on a differential element within a solid shows that heat transfer must satisfy the basic differential equation:

$$\frac{dT}{dt} = \alpha \frac{d^2T}{d\ell^2} = \frac{k}{\rho c_p} \frac{d^2T}{d\ell^2} \qquad (1)$$

where

- k = thermal conductivity of the solid
- ρ = density of the solid
- c_p = specific heat of the solid
- α = thermal diffusivity of the solid (= $k/\rho c_p$ by definition)
- t = time of heat transference
- dT = differential temperature in the solid
- $d\ell$ = differential distance at the point of differential temperature

Also, if there is a non-negligible thermal resistance between the surface of the solid and its environment, the solution to equation (1) must simultaneously satisfy the boundary equation

$$q = U\Delta T \qquad (2)$$

where

- q = heat flux at the surface
- U = overall heat transfer coefficient
- ΔT = temperature difference across the boundary resistance

Consider a solid which is a nonheat-producing, homogeneous rectangular parallelepiped at a uniform temperature, T_O. If it is exposed to a uniform temperature, T_A ($\neq T_O$), then for the rectangular coordinate system originating at the center of the solid (fig. 4), the solution[5] satisfying equations (1) and (2) has been found to be

[5] Bird, R. B., W. E. Stewart, and E. N. Lightfoot. Transport Phenomena. 1960, p. 352. Wiley, N.Y.

[6] The actual solution is an infinite series solution which after sufficient time will have negligible terms after the first term such that they can be omitted, leaving equation (3).

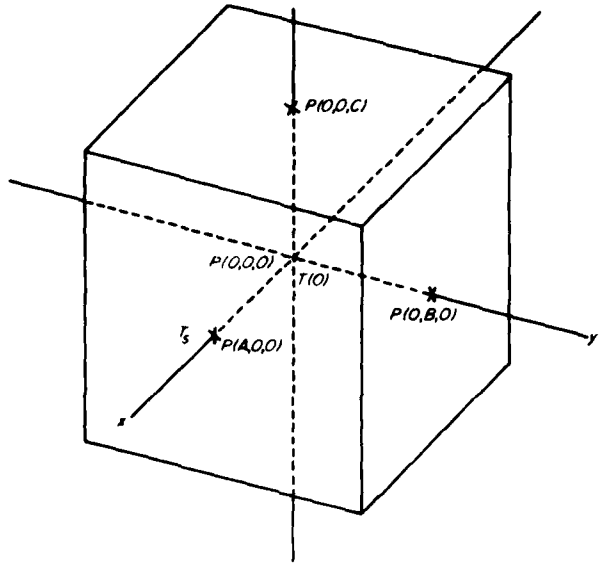

Figure 4 — Rectangular coordinate system as applied to a package for determination of thermal properties

(M 149721 2)

$$\frac{T_A - T(x,y,z)}{T_A - T_O} = \frac{2\,H_A \cos \lambda_A X}{[(H_A^2 + \lambda_A^2)A + H_A]\cos \lambda_A A} e^{-\lambda_A^2 \alpha t}$$

$$\times \frac{2\,H_B \cos \lambda_B Y}{[(H_B^2 + \lambda_B^2)B + H_B]\cos \lambda_B B} e^{-\lambda_B^2 \alpha t} \qquad (3)$$

$$\times \frac{2\,H_C \cos \lambda_C Z}{[(H_C^2 + \lambda_C^2)C + H_C]\cos \lambda_C C} e^{-\lambda_C^2 \alpha t}$$

where

- $\frac{T_A - T(x,y,z)}{T_A - T_O}$ = unaccomplished temperature change, $T_r(x,y,z)$
- T_A = bulk environment temperature
- $T(x,y,z)$ = temperature at a point P(x,y,z) in the solid
- T_O = initial temperature of the solid
- $H_{A,B,C}$ = U/k for the mutually perpendicular sides A,B,C
- $\lambda_{A,B,C}$ = positive first roots of the equation $H_L = \lambda_L \tan \lambda_L L$; L = A,B,C
- X,Y,Z = axial distances to the point P(x,y,z)
- A,B,C = axial distances from the center to the surfaces of the sides
- e = natural exponential
- t = elapsed exposure time to T_A

Application

A. General Technique for Finding Overall Thermal Resistance, R, at Surface of Solid

Simultaneously measure the outside air temperature together with the solid temperature at two points along the same axis and on the same side of the origin. Then,

algebraic manipulation[9] of equation (3) gives

$$\frac{T_A - T(x_1,0,0)}{T_A - T(x_2,0,0)} = \frac{\text{Cos } \lambda_{x_1} X_1}{\text{Cos } \lambda_{x_2} X_2} \qquad (4)$$

at the time of the temperature measurement.

Let the two points in the solid be P(A,O,O) and P(O,O,O), P(O,B,O) and P(O,O,O), or P(O,O,C) and P(O,O,O). Equation (4) becomes

$$\frac{T_A - T_S}{T_A - T(0)} = \text{Cos } \lambda_L L \qquad (5a)$$

or rearranging

$$\lambda_L = \text{Cos}^{-1}[(T_A - T_S)/(T_A - T(0))]/L \qquad (5b)$$

where

λ_L = root of equation $H_L = \lambda_L \tan \lambda_L L$
T_A = bulk air temperature on side of the solid
T_S = surface temperature at the axis of the solid
T(O) = center temperature of the solid
L = distance from center of the solid to the surface along the axis

From the definition of λ and by knowing the thermal conductivity of the solid, one can calculate the heat transfer coefficient, U, and the thermal resistance, R:

$$H_L = \lambda_L \tan \lambda_L L \qquad (6)$$

$$U = kH_L = k\lambda_L \tan \lambda_L L = R^{-1} \qquad (7)$$

B. General Technique for Finding Thermal Diffusivity, α, of Solid

By letting P(x,y,z) = P(O,O,O), in equation (3), cos $\lambda_L L$ = 1. Taking the natural logarithm of equation (3) and condensing one gets:

$$\ell n T_f(O) = \ell n \left(\frac{T_A - T(O)}{T_A - T_O}\right) = C_1 - (\lambda_A^2 + \lambda_B^2 + \lambda_C^2)\alpha t \qquad (8a)$$

$$= C_1 - (\Sigma\lambda^2 \times \alpha)\, t \qquad (8b)$$

where

C_1 = constant = intercept
$\lambda_{A,B,C}$ = λ-values for mutually perpendicular sides

$\frac{T_A - T(O)}{T_A - T_O}$ = unaccomplished temperature change at center of solid, $T_f(O)$

This is a linear relationship. The thermal diffusivity will be the negative of the slope when $\ell n T_f(O)$ is plotted against $(\lambda_A^2 + \lambda_B^2 + \lambda_C^2)t$ (eq. 8a).

This theory and these techniques for determining the overall heat transfer coefficient and thermal diffusivity have been known and applied for several decades, but have required extensive time to collect and analyze the data. Using today's electronic data collection devices coupled with computer processing, minimal time and effort is needed.

C. Modification of General Techniques for Determining Resistance and Diffusivity in a Corrugated Fiberboard Package

A homogeneous product packed tightly in a corrugated fiberboard box can be described as a solid rectangular parallelepiped. It will have three surface thermal resistances in series: (1) R_1, an inner air resistance between box and solid arising from imperfect contact; (2) R_2, the resistance due to the boxboard itself; and (3) R_3, an outer air resistance between the box and the bulk air. The composite resistance is related to the overall heat transfer coefficient, U:

$$U = \frac{1}{R_1 + R_2 + R_3} = \frac{1}{R_{overall}} \qquad (9)$$

To apply the theory outlined, the temperature at the interface between the inner air layer and the product surface is needed—a measurement almost impossible to achieve. A thermocouple sandwiched between the product and the corrugated container would only give the average temperature of the inner air layer. Subsequent application of equations (5b) and (8) would only give apparent heat transfer coefficients and thermal diffusivities and not necessarily the true values.

If $\ell n T_f(O)$ is plotted against time (eq. 8), the slope of the line would be $-(\Sigma\lambda^2 \times \alpha)$. This slope will be nearly constant since both time and $\ell n T_f(O)$ are known accurately and $\ell n T_f(O)$ is independent of the interface. Therefore, it is obvious that

$$(\Sigma\lambda^2 \times \alpha)_{true} = (\Sigma\lambda^2 \times \alpha)_{apparent} \qquad (10)$$

From equation (10), then,

$$(\Sigma\lambda^2)_{true} = \frac{(\Sigma\lambda^2 \times \alpha)_{apparent}}{\alpha_{true}} \qquad (11)$$

Thus, for determining the true heat transfer coefficient equation (8b) can be applied directly to determine the term $(\Sigma\lambda^2 \times \alpha)_{apparent}$ with division by the true diffusivity; or one can apply equation (5b) then equation (8a), and calculate the term $(\Sigma\lambda^2 \times \alpha)_{apparent}$ with subsequent division by the true diffusivity. While the former technique is straightforward, the latter method allows one to determine the magnitude of the original approximation of the heat transfer coefficient and diffusivity.

[9] Carslaw, H. S., and J. C. Jaeger. Conduction of Heat in Solids. 1959, p. 186. Oxford Press, London.

For this study the latter technique was selected as the true diffusivity can be determined through extrapolation of the apparent values.

Appendix II—Experimental Procedure

System Description

A. The solid used was commercial 454-gram flat-packs of margarine consisting of four 113-gram sticks wrapped in greaseproof paper and packaged in a paper-board box. This solid is relatively homogeneous and retains its physical properties essentially constant over the temperature range employed. Margarine is also representative of actual commercial loads. The flat-packs allow for variable stacking patterns. In this study, four packages were stacked to form a cube having approximately 130-mm sides.

B. Corrugated boxes were fabricated from 205-127C-205 corrugated sheetstock. Inner flaps were cut to meet tightly, and outer flaps were cut back to just form an edge seal (flap length of 12.7 mm). Box thickness at the center of the panels was equal on all sides. For greater board thicknesses, larger boxes had smaller boxes nested inside, with filler sheets of corrugated employed in the voids.

C. The environment was provided by two adjacent temperature-humidity rooms: one at 23° C, 50 percent relative humidity and the other at -26° C. An insulated window between the two rooms allowed access.

D. Air flow was provided by a fan which was adjusted such that the air stream would strike the package normal to its front. Air velocities were measured at the front face of the package and the fan speed was adjusted to the desired level accordingly.

E. Thermocouples were located at the center of the margarine, at the centers of the six interfaces between margarine and box, and in the bulk air 25.4 mm from each surface, all along the axes.

F. The package rested on 12.7-mm-diameter dowels set in a framework supporting the thermocouples used to measure air temperatures. The framework with package was passed between rooms without disturbing the relative positions of the thermocouples.

G. A programmable data acquisition system would periodically scan the thermocouples. Combined scan-output time was approximately 20 seconds with actual scanning time being much less.

Procedure

A. Data Collection

Thermal equilibrium was established in the package. An initial scan just prior to starting the run gave the initial temperature, T_O. With the fan on, the package and framework were quickly subjected to a step increase in bulk air temperature by being transferred to the adjacent room through the access panel in the common wall. The data acquisition system was activated at time zero. Temperature scans were taken until the center temperature approximated the bulk air temperature. Scan intervals were adjusted periodically to reflect rate of temperature change, and approximately 100 scans per test were collected. When the package temperature had again equilibrated, the frame and package were brought back into the original room and a second set of data was recorded. By this method both heating and cooling data were collected for each test package and air velocity.

B. Data Processing

Initial data processing consisted of calculating $\frac{T_A - T_S}{T_A - T(O)}$ and $\ell n T_r(O)$ for use in equations (5b, 6, and 8). These values were determined for each side of the package and for each time scan.

Since the study was intended to determine an average value for U which would be indicative of box behavior, the next processing step integrated the time-smoothed values of λ_n and calculated for each side of the package an average $\bar{\lambda}_n$ according to the formula (fig. 3A,B):

$$\bar{\lambda}_n = \frac{\Sigma_O^t \lambda_n(t)\Delta t}{\Sigma_O^t \Delta t} \qquad (12)$$

From $\bar{\lambda}_n$, $\bar{H}_n$ was determined by equation (6). The overall apparent $\bar{\lambda}$ and $\bar{H}$ for the box was calculated by averaging the six $\bar{\lambda}_n$ and $\bar{H}_n$ values.

Calculation of the apparent thermal diffusivity was more complicated. In order to determine the slope (eq. 8), the value of $\Sigma\lambda^2 = (\lambda_X^2 + \lambda_Y^2 + \lambda_Z^2)$ needed to be known; but for each side x and its corresponding λ_X there are four combinations of λ_Y and λ_Z. Therefore all four $\Sigma\lambda_i^2$ were determined and averaged. Once this was done $\ell n T_r(O)$ could be plotted verses $(\Sigma\lambda_i^2)t$. An algorithm was then applied to find the linear region of the data. From here the slope was found. This process also was repeated for each side (fig. 5). The six values of apparent thermal diffusivity were averaged as the solid was not perfectly homogeneous.

The final output gave the apparent thermal diffusivity, and the apparent values of $\bar{\lambda}_n$ and $\bar{H}_n$ for each of the six sides of the package followed by the overall averages of the six sides, including standard deviations and coefficients of variation among the sides. These values constituted the data used for the initial analysis of the effects due to air velocity and board thickness.

C. Determination of Thermal Conductivity of Margarine Flatpacks

The data processing yields values of H, which is the ap-

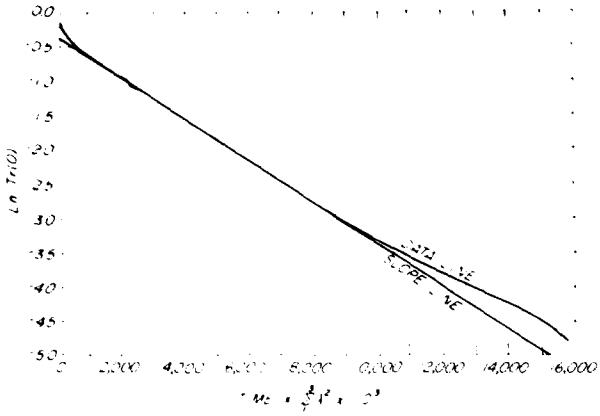

Figure 5 — Determination of the apparent thermal diffusivity of the packaged product (margarine). The "Slope" line approximates the linear region of the "Data" line. The apparent thermal diffusivity of the margarine equals the absolute value of this slope

M 149721-4

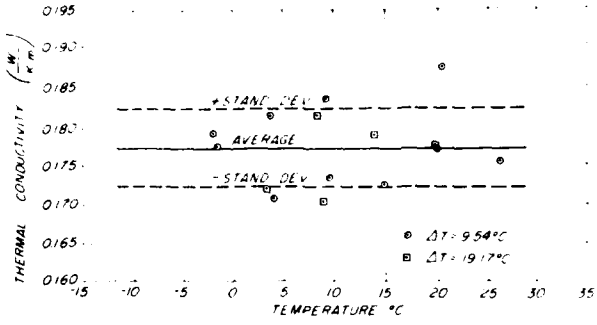

Figure 6 — Thermal conductivity of boxed margarine using a guarded hot plate apparatus. Standard deviation equaled 0.005 W/K•m. Coefficient of variation was 2.8 percent

(M 149721-3)

parent overall heat transfer coefficient divided by the thermal conductivity of the margarine, U/k. To determine U, it was necessary to first determine k. This was accomplished using a commercial thermal conductivity tester calibrated against a National Bureau of Standards glass fiber standard and based on the ASTM C-518 procedure. Flatpacks of margarine, 31.8 mm thick, were used as the test sample. Two temperature differentials were employed: 9.5° C and 19.2° C. The data are presented in figure 6. The scatter was about equal for both temperature gradients. For the temperature range in this study the thermal conductivity only varied about 2.5 percent from 0.1744 W/K•m at -26° C to 0.1786 W/K•m at 27° C. This permitted the use of the average conductivity which was 0.176 W/K•m with a standard deviation of 0.005 W/K•m and a coefficient of variation of 2.81 percent.

D. Determination of True Thermal Diffusivity of Margarine

To obtain the true thermal diffusivity the data for margarine alone (no package) was employed (fig. 7). Only the cooling data was used, as the thermal resistance was lower than for heating. Extrapolation to zero reciprocal air velocity gives the diffusivity at infinite air velocity where the outer boundary resistance would theoretically cease to exist. A linear regression of the three points gives an intercept value of 9.406 x 10^{-8} m²/s. This value was assumed to be the true thermal diffusivity of the product. Applying equation (11) in the following form gives the true λ-value:

$$(\lambda_x^2 + \lambda_y^2 + \lambda_z^2) = \frac{[(\overline{\lambda_x^2} + \overline{\lambda_y^2} + \overline{\lambda_z^2}) \times \alpha]\ \text{apparent}}{\alpha\ \text{true}} \qquad (13)$$

Since the composite λ-value was calculated to represent the package as a whole:

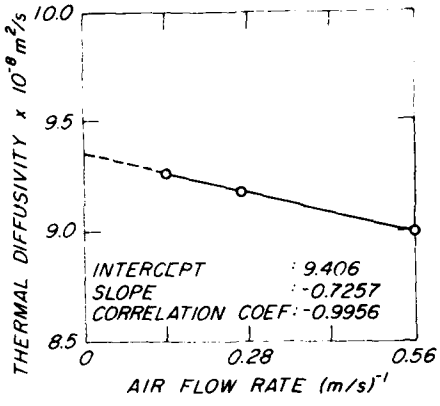

Figure 7 — Determination of true thermal diffusivity of packaged margarine. Extrapolation of data to 0 (m/s)$^{-1}$ gives thermal diffusivity for a perfectly mixed heat source or sink which is the true thermal diffusivity of the product

(M 149721-1)

$\lambda_x = \lambda_y = \lambda_z = \lambda$, the true average λ-value

and $\overline{\lambda_x} = \overline{\lambda_y} = \overline{\lambda_z} = \overline{\lambda}$, the apparent average λ-value

and equation (13) becomes

$$3\,\lambda^2_{\text{true}} = \frac{(3\,\overline{\lambda^2} \times \alpha)\ \text{apparent}}{\alpha_{\text{true}}} \qquad (14a)$$

or,

$$\lambda_{\text{true}} = \overline{\lambda} \times \left(\frac{\alpha\ \text{apparent}}{\alpha_{\text{true}}}\right)^{1/2} \qquad (14b)$$

E. Final Data Calculation
Using equations (14b and 6), plus the output from the initial data processing, plus the true diffusivity, one gets the desired resistance for the various board thicknesses and air velocities. The resistance values at each thickness were then plotted versus reciprocal air velocity and linear regression lines were calculated using 0.09 m/s as an estimate of 0 m/s (table 2). These data were extrapolated to 0 $(m/s)^{-1}$ for the infinite air velocity values for table 1 and figure 1.

Appendix III—Hypothesis Concerning Differences In Heating and Cooling Behavior

Situation 1—Heating of Solid Product
When heating the product, thermal energy moves from the bulk air through a semistagnant air film layered between the bulk air mass and the box. This boundary layer will have a finite effective thickness and a thermal gradient, and thus also a density gradient. As the bulk air velocity increases, this film thickness decreases and correspondingly its thermal resistance decreases. This is evident on figure 1 where line II is less than line III. Also, as the board thickness is reduced, the overall thermal resistance decreases and the overall thermal flux increases. In the absence of sufficient air mass movement to re-supply the energy draining from the bulk air, that part of the bulk air adjacent to the outer edge of the stagnant air layer will cool and itself become part of the stagnant layer, i.e., the stagnant layer thickens and its resistance value increases. This is evident in figure 1, line III-a, where the difference in resistance between lines III-a and II increases even though the overall resistance (line III-a) is decreasing.

On the other hand, an increased air velocity maintains the necessary bulk thermal energy source. The increased velocity will stir the outer edge of the stagnant air layer making it thermally more uniform with the bulk air, thereby effecting a reduction in the thickness of the remaining air layer and its corresponding resistance. The overall resistance, line III, would converge on line II. Examination of the data of table 1 for any board thickness and for the different air velocities shows this effect. The key point is that a change in thickness of the outer stagnant air boundary layer due to the presence or nonpresence of air flow has a significant effect on overall resistance.

Situation 2—Cooling the Solid Product
For the opposite case, cooling, an entirely different mechanism may be taking place. With the outward heat flux there will be a reversal of the temperature gradient across each resistance zone relative to heating and a corresponding reversal of the density gradient of the outer boundary air layer. This situation places the lower density air adjacent to the board. As in the case of heating, at the greater board thicknesses the thermal flux is sufficiently low that the air film will remain relatively undisturbed and the resistance behaves as for heating. For the lower range of board thickness the overall resistance is lower, as it was for heating. However, the higher outward thermal flux accompanying this lower resistance may cause thermal hot spots to develop at high points of the board-air interface. Because of the heterogeneous nature of the surface, these hot spots, located at the fiber tips, may be the source of thermal convection currents. These currents may tend to disrupt the air film bond at the board surface, thereby allowing the layer to be virtually stripped away by even a minimal bulk air flow, decreasing the overall resistance. As the board thickness is reduced further the rate of convective transfer will increase due to increased flux and the resistance III-b of the stagnant layer decreases relative to resistance III-a. If the flux is sufficiently high, the entire stagnant layer nearly ceases to exist and the resistance values approach those for infinite air velocity line II.

To show that there is actually a mechanistic difference between heating and cooling, one need only examine the time histories (fig. 3) for a no-air-flow single-wall box. The value "λ" is reflective of the overall heat transfer coefficient and thus the reciprocal of the overall resistance. At the beginning of the heating run (fig. 3- B) there is a large inward thermal flux due to the large overall temperature difference. The high flux disrupts the air layer almost completely, giving high heat transfer efficiency, shown by the high values of "λ" at the beginning of the run. As the overall temperature difference between bulk air and product decreases with time, so does the overall flux. The disturbance of the outer air layer lessens and the layer effectively thickens, thereby increasing its resistance and decreasing the flux even further. This is evidenced by the rapid decrease in "λ." For cooling (fig. 3-A) the layer is sufficiently thin due to the postulated convective effect that the resistance stays nearly constant and at a low level, as is evidenced by the higher value of "λ" throughout the run. The shapes of these curves are typical of all runs made, varying only in accordance with the mechanism proposed.

Acknowledgment

The author wishes to thank David P. Schroeder for his technical assistance in the fabrication and maintenance of the experimental equipment and for performance of the experimental phase of the study, and Wencil W. Wlodarczyk for computer programming and data processing.

CON 2-1

Forest Products Laboratory

Overall Effective Thermal Resistance of Corrugated Fiberboard Containers, by David W. Bormett, Madison, Wis., FPL 1981.
12 p. (USDA For. Serv. Serv. Res. Pap. FPL 406).

While the mechanical properties of corrugated fiberboard are known, little knowledge has been available on its thermal properties. Here the thermal resistance of a container was determined as a function of air velocity and board thickness, and an appropriate design curve is presented.

Keywords: Corrugated containers, heat transfer coefficient, thermal resistance, corrugated fiberboard, wind speed.

2,0-13-9/81

☆ U. S. GOVERNMENT PRINTING OFFICE: 1981/750-027/21


DATE
ILME